

Spectroscopic study of low-velocity charge-exchange collisions of S^{7+} ions with H_2 and He targets

M. Cornille

Observatoire de Meudon, 92190 Meudon, France

T. Ludac, D. Hitz, and S. Bliman

Service de Physique Atomique, Département de Recherche Fondamentale, Centre d'Etudes Nucléaires de Grenoble, Boîte Postale 85X, 38041 Grenoble, France

G. A. Heckman and E. J. Knystautas

Département de physique, Université Laval, Laval, Québec, Canada G1K 7P4

(Received 6 September 1988; revised manuscript received 16 January 1990)

The far-uv spectra of sodiumlike S VI and neonlike S VII are obtained following single- and double-electron capture into excited states of slow (~ 10 -keV/ q) S^{7+} ions passing through thin H_2 and He gas targets. The high charge-state and excited-state selectivity of the collision process facilitated line identification. New model-potential calculations using the SUPERSTRUCTURE code are compared with measurements for S VII. Changes in relative line intensities observed using the different target gases help to elucidate the collision mechanism via the relative initial-state populations. Capture takes place into n states as predicted by a classical model, while the distribution among l states is nonstatistical at this velocity (~ 0.29 a.u.).

I. INTRODUCTION

The capture of electrons from stationary gas targets by multiply charged low-velocity ions is of interest from a fundamental point of view as well as for an understanding of basic processes in thermonuclear and astrophysical plasmas.¹ In addition, capture into excited states of ions of the neon isoelectronic sequence holds some promise in eventual schemes for x-ray lasers.²

Recent spectroscopic studies of the neon sequence (Refs. 3–6) have used laser-produced plasmas and beam-foil spectroscopy. In the present work, low-velocity S^{7+} ions capture electrons from hydrogen and helium gas targets into excited states of the neonlike sulfur ion. The light that is subsequently emitted by the spontaneously deexciting projectiles has a negligible Doppler effect due to the low velocity of the ions, and usually originates from a single, or at most two, ionic species, due to the high charge-state (and also excited-state) selectivity of the capture process.

Line identification is facilitated by isoelectronic sequence comparisons and by the differential excitation probabilities for excited states that are available by use of two different target gases. The results obtained herein are also compared with new calculations of the S VII system using a model potential. In turn, knowledge of the energy levels and calculated decay rates coupled with measured line intensities can provide information about relative initial-state populations (both n and l), which are needed to understand the dominant mechanisms for single- and double-capture collisions.

Previous work in this area has dealt mostly with electron capture by either bare ions or those with closed shells. The case of open-shell ions can lead to additional

complexity in the collision process and is an area yet unexplored by theory. In the few experimental studies performed for such ions, it was necessary to first calculate hitherto unavailable energy levels and wavelengths associated with doubly excited states.^{7,8}

II. EXPERIMENTAL CONDITIONS

These have been described elsewhere⁹ in a general way and are summarized here along with a description of new features. Ions of S^{7+} emanating from the MINIMAFIOS (Ref. 10) electron cyclotron resonance ion source are accelerated to 10 keV/ q and pass into the target chamber after mass and charge filtering by two magnetic analyzers in tandem, having a resolution of 0.036 amu.

The collision chamber is filled with hydrogen or helium gas at a pressure of 5×10^{-5} mbar (measured with a capacitance manometer), which is known from previous work to ensure single-collision conditions.

Following single- and double-electron capture into excited states of the neonlike and sodiumlike ion, respectively, spontaneously emitted photons are dispersed by a 1 m grazing incidence (85°) vuv monochromator "GISMO" (with a 1200 lines/mm grating) and detected with a channel electron multiplier. The 400- μ m-wide entrance slit is located 53 cm from the scattering center and admits photons emitted at 25° to the forward direction. The acceptance solid angle has been measured to be 0.3 μ sr. Photons emerging from the 400- μ m exit slit are wavelength scanned by displacing the detector. For survey spectra such as are shown herein, each channel represents approximately 1 Å, the scanning speed depending on the time required to collect a preset charge (~ 30 μ C) in each channel.

III. MODEL-POTENTIAL CALCULATIONS

Since the energy levels of the neon sequence are still known in a rather fragmentary fashion, especially for the

higher n states, it seemed useful and appropriate to calculate these with a modern code and compare their values with measured ones from various sources. A relativistic program¹¹ called SUPERSTRUCTURE, which had already

TABLE I. Calculated mean wavelengths and multiplet transition probabilities for $2p^53l-2p^5nl$ ($n=4,5$) manifolds in S VII.

Transition	λ (Å)	A (10^8 sec^{-1})	Transition	λ (Å)	A (10^8 sec^{-1})
$3s-4p$			$3s-5p$		
$^1P-^3P$	210.52	15.0	$^1P-^1S$	153.81	20.8
$^3P-^3S$	208.78	73.0	1D	157.36	41.1
1P	206.21	53.8	$^3P-^3S$	156.86	50.4
3P	204.33	42.3	1P	156.23	41.6
3D	206.22	55.8	3P	155.24	36.0
			3D	155.99	42.2
$3p-4s$					
$^1S-^1P$	388.45	19.4	$3p-5s$		
$^1P-^1P$	300.86	20.3	$^1D-^3P$	200.04	17.0
$^1D-^1P$	303.91	101	$^3P-^1P$	200.06	31.2
$^3S-^3P$	286.77	21.5	3P	198.64	20.9
$^3P-^1P$	300.68	33.2	$^3D-^1P$	195.62	45.6
3P	309.93	47.9	3P	194.26	36.1
$^3D-^3P$	299.41	109			
$3p-4d$			$3p-5d$		
$^1S-^1P$	277.60	66.8	$^1S-^1P$	206.84	84.1
$^1D-^1F$	236.40	88.3	$^1D-^1F$	181.59	70.5
$^3S-^3P$	227.43	46.7	$^3S-^3P$	175.74	28.3
$^3P-^1P$	229.69	18.5	$^3P-^1P$	179.02	25.9
3P	241.75	32.1	3P	184.17	27.4
3D	237.26	70.0	3D	182.41	56.1
$^3D-^1D$	233.49	83.6	$^3D-^1D$	172.92	59.6
3F	233.27	75.6	3F	179.92	56.2
$3d-4p$					
$^1P-^1S$	437.10	35.3	$3d-5p$		
$^1F-^3P$	442.34	16.7	$^1P-^1S$	268.48	30.5
$^3P-^3S$	439.45	40.3			
$^3D-^3P$	458.07	17.5	$3d-5f$		
1D	447.50	36.3	$^1P-^1D$	256.21	55.3
$^3F-^1P$	438.32	25.5	$^1D-^1F$	248.36	27.3
3D	438.36	31.7	3G	244.97	25.0
			$^1F^3F$	244.51	52.2
$3d-4f$			1G	244.77	18.6
$^1P-^1D$	385.84	87.3	$^3P-^3D$	235.19	71.6
3D	386.88	19.4	3F	237.58	31.9
3F	377.17	31.7	1G	237.83	31.9
$^1D-^1D$	355.34	25.0	$^3D-^1D$	243.15	60.3
1F	345.77	59.3	3D	246.61	56.4
3G	348.39	67.3	3F	249.24	25.9
$^1F-^3D$	348.19	31.3	3G	245.75	40.9
1G	348.14	51.7	$^3F-^1F$	240.58	112
$^3P-^1D$	333.53	47.5	3F	240.66	18.9
3D	334.31	159	1G	240.91	116
3F	327.03	23.6	3G	237.40	70.4
$^3D-^1D$	356.98	129			
3D	357.87	42.3			
3G	349.96	108			
$^3F-^1D$	339.63	63.4			
1F	339.12	308			
3F	332.89	36.3			
1G	340.39	307			

been tested in this capacity,¹² was used in the present work. This code uses a model potential and is of the Thomas-Fermi-Dirac type. Taking into account the averaged repulsion of all the other electrons, the method used leads to a central potential $V(r)$ that satisfies the simple boundary conditions

$$V(r) = \begin{cases} Z/r, & r \rightarrow 0 \\ (Z-N+1)/r, & r \rightarrow \infty, \end{cases} \quad (1)$$

where Z is the nuclear charge and N is the number of electrons. Energy levels are calculated using multiconfigurational wave functions and some of the Breit-Pauli corrections are introduced into the Hamiltonian by a perturbational approach. A scaling parameter Λ_l ensures that all radial functions with the same l are calculated in the same potential and hence orthogonal, given $V(r) = V(\Lambda_l, r)$.

All energy levels (103 in all) arising from configurations $1s^2 2s^2 2p^5 nl$ (nl ranging from $2p$ through $5f$) were calculated, as well as wavelengths and transition probabilities for all allowed electric-dipole transitions arising between the levels. (The electric-quadrupole and magnetic-dipole transitions were also calculated, but not used in the present work.)

Results of the calculations are shown in Table I, where each multiplet is characterized by a mean wavelength and a multiplet transition probability, the former obtained using the center of gravity of the upper and lower term energies.

IV. RESULTS AND DISCUSSION

Figures 1 and 2 show the spectra obtained in the region 190–1070 Å with hydrogen (molecular) and helium targets under single-collision conditions. Eight spectra were spliced together, and through overlapping lines the peak amplitudes could be adjusted to a common scale. By using several pairs of lines arising from common upper levels in highly charged carbon, nitrogen, and oxygen ions, a relative response curve of the spectrometer and detection system was determined over a wide wavelength range (approximately between 200 and 1000 Å). Thus the relative line intensities for a given target gas are significant over the entire spectral range, we would estimate, to within 20%. (The rise in background at the extreme left-hand side of Fig. 1 is an artifice due to extrapolation into the shortest wavelength range.)

Most identifications of S VII lines originating on levels with $n > 3$ were made using the model-potential calculations, even though the instrumental resolution was sufficient to distinguish only one, or a few, multiplet components. All designations are given in LS coupling, although jK coupling would be more appropriate for some of the higher levels (see Refs. 4 and 13). The S VII $4f-5g$ yrast transitions are near the hydrogenic values and the assignments come from unpublished work of the Lund group.⁶ Assignments for the $3-3$ transitions (Fig. 2) are based on the thorough analysis of Kononov *et al.*³ using a laser-produced plasma. A similar source was used by Jupén *et al.*⁴ to unravel the $3d-4f$ manifold (Fig. 1). The $3-4$ and $3-5$ transitions are mostly unknown. Table I

shows the results of the model-potential calculations. The sodiumlike system seems to be in much better shape, and all the S VI lines compiled by Kelly¹⁴ in the relevant wavelength region have been observed, although some comments about the S VI lines observed are considered below.

A striking feature of the spectra shown is the very high charge-state selectivity of this collision process. All lines are attributed to S VII, which corresponds to one-electron capture, or to S VI (two-electron capture). The S VI lines are relatively weaker in the helium gas target case. No lines appear from levels with $n > 5$. Furthermore, lines arising from $n = 5$ levels are very strongly attenuated in passing from the molecular hydrogen to the helium target, implying that there is also an excited-state selectivity present. The principal quantum number n_p of the recom-

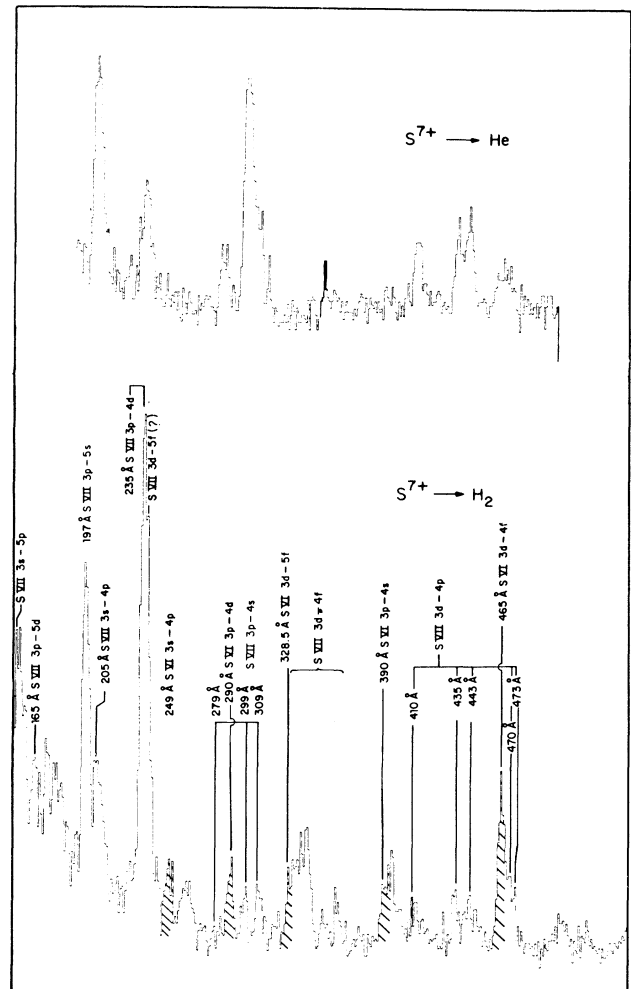


FIG. 1. Spectra of S^{7+} ions following single- and double-electron capture from thin He and H_2 targets. (The cross-hatched peaks represent two-electron capture to the S^{5+} ion. See text for discussion of peaks identified with a question mark.) These and the following spectra have been corrected for spectrometer and detector response.

bined projectile is related to the charge of the incoming ion and to the ionization potential of the target. The "classical overbarrier transition model" (see, for example, Ref. 15) yields an effective upper limit to n_p after a one-electron transfer:

$$n_{p1}^2 \leq \frac{Q^2}{\frac{2I_1}{27.2} \left[1 + \frac{Q-1}{2\sqrt{Q}+1} \right]}, \quad (2)$$

where I is the ionization potential of the target in eV and Q is the incident ion charge. In the present case, this corresponds to an $(n_p)_{\max}$ of 3.7 for helium and about 4.7 for the molecular hydrogen target, which is borne out by the data. A similar relation holds for the case where two electrons are captured:

$$n_{p2}^2 \leq \frac{(Q-1)^2}{\frac{2I_2}{27.2} \left[1 + \frac{Q-2}{2\sqrt{Q-1}+1} \right]}. \quad (3)$$

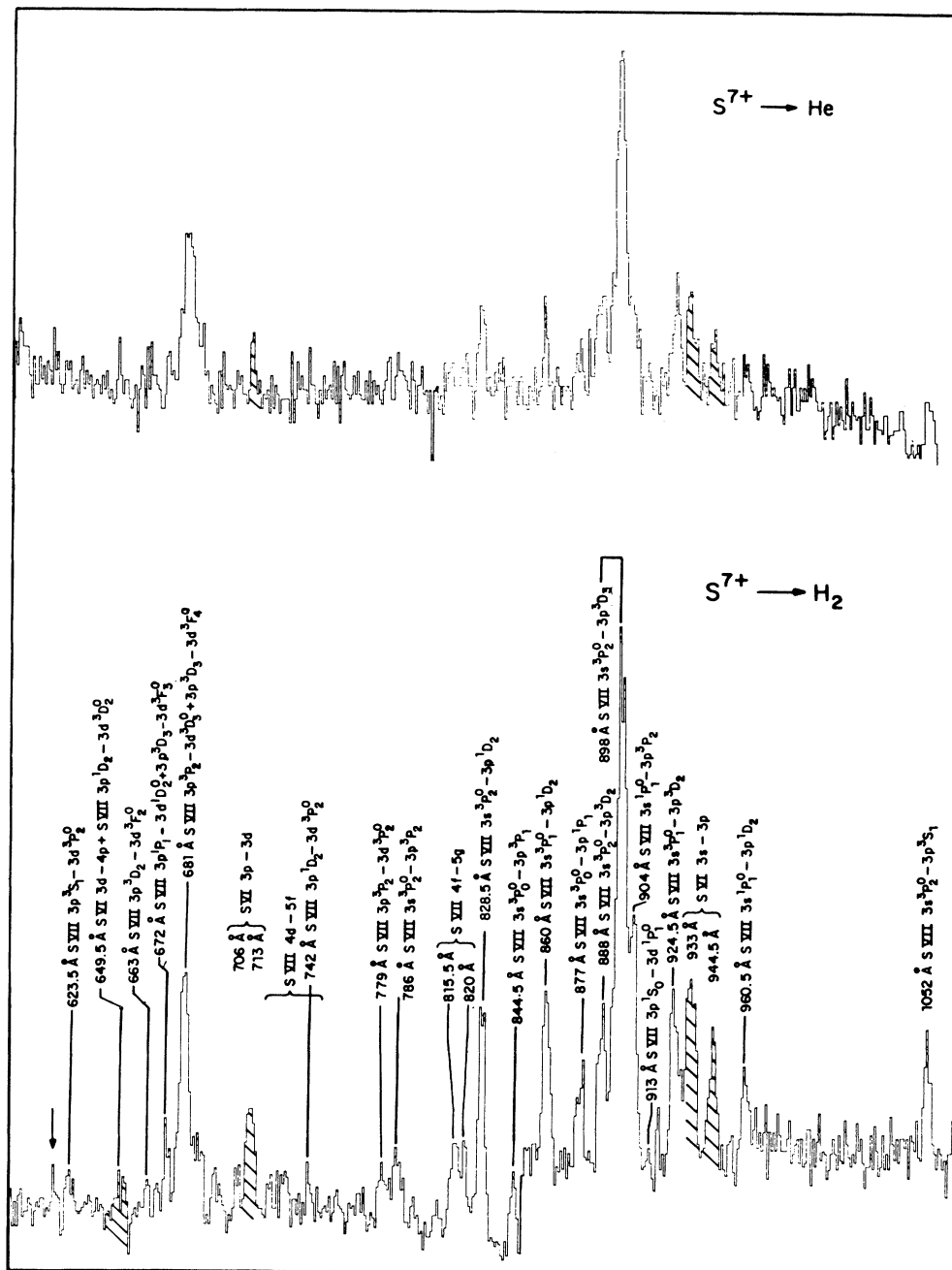


FIG. 2. Spectra of S^{7+} ions following single- and double-electron capture from thin He and H_2 targets. The 3-3 line identifications are from Kononov *et al.* (Ref. 3). The feature at 614 Å discussed in the text is indicated by the arrow.

It should be kept in mind that a first capture leaves the ion in a Ne-like state. The radiative decay of the Ne-like ions in 3L states ends up in $2p^5 3s {}^3P_{0,2}$ long-lived metastable states. It is understood that a capture on this ion would end up in $(2p^5 3s {}^3P_{0,2})n'l' {}^{2,4}L$. These states may either autoionize and/or decay radiatively. The radiative stabilization wherein the $3s$ electron closes the $2p^5$ subshell would be subsequently followed by a further decay in the $n'l'$ electron to a normal 2L level of the Na-like isoelectronic sequence.¹⁶

Not all the 3-3 transitions given in Ref. 3 are observed. Some of the latter are uncertain. Furthermore, the radically different nature of the excitation mechanism must be considered. Cascade pathways will also strongly affect relative intensities in the present work. In the helium target case, capture takes place preferentially in $n=4$ states, $n=3$ being populated by cascading. Yrast or near-yrast transitions will decay via $3d$, while $3d$, $4d$, $3s$, and $4s$ will decay to $2p^6$, and from branching ratio considerations the np states will go through $3s$ rather than $3d$. For the molecular hydrogen target, capture into $n=5$ dominates, the f and g states will cascade down the yrast chain and be funneled through $3d$, while $4d$ and $5d$ will preferentially decay to the ground state rather than to $3p$.

Very recent work¹⁷ by the Lund group suggests that a weak feature at 614 \AA (indicated by an arrow in Fig. 1) is the transition between core-excited states $2p^5 3s 3p {}^4D_{7/2} - 2p^5 3s 3d {}^4F_{9/2}^0$ in sodiumlike S VI. If confirmed, this would not be inconsistent with two-electron capture into excited states described by the above model. (The quartet states in question lie above the first autoionization limit, but since Coulomb autoionization cannot take place for these states in pure LS coupling, they autoionize weakly, hence the branching ratios are such that the possibility exists of observing radiative decay from the upper level.)

Turning to the l -state distributions of the initial populations, large uncertainties are introduced by the fact that the neonlike multiplets contain many lines that are inevitably blended. Thus the $3s-4p$ and $3d-4p$ manifolds contain over 100 lines for each of which we have calculated transition probabilities. Not only are the lines spread out in wavelength over tens of angstroms, but uncertainties in transition rates are difficult to estimate (agreement between results of dipole-length and dipole-velocity formulations providing only a rough guide), so that quantitative estimates of l distributions are not yet fully feasible, however qualitative estimates are given below. This is in contrast to previous work where the simple level structure associated with systems of two or three active electrons allowed such calculations.

In spite of these difficulties, qualitative features of the spectra shown in Figs. 1 and 2 show that the distribution of l states is far from statistical, in that all yrast transitions are anomalously weak. For the helium target case in Fig. 1, for example, the $3d-4f$ yrast transitions are almost completely suppressed, the spectrum being dominated by lines emanating from $4s$ and $4p$ multiplets. At approximately the same velocity, observation of $\text{Ar}^{9+} + \text{H}_2$ in the $30\text{--}55\text{-\AA}$ wavelength range shows that the spectrum is dominated by $2p^5 3s {}^{1,3}P_1 - 2p^6 {}^1S_0$ around

$48\text{--}49 \text{ \AA}$, whereas $2p^5 3d {}^{1,3}P_1 - 2p^6 {}^1S_0$ around 42 \AA is extremely weak. This provides evidence for the fact that a small fraction of the population has gone into $3d {}^{1,3}P$ states, whereas most of the capture has taken place into the $np {}^{1,3}P$ states. These states are forced to cascade down to $3s {}^{1,3}P$ states.¹⁶ This behavior is also responsible for intensity that is higher in the $3s-3p$ transition manifolds than in the $3p-3d$ transition manifolds. In these circumstances $3d$ is fed by cascades from states of higher angular momentum such as f and g . This is clearly seen in Fig. 1, where for $\text{S}^{7+} + \text{He}$, the most intense transition manifold is $3s-4p$ (the latter decaying to both $3s$ and $3d$); $4s$ heavily feeds $3p$, whereas $4d$ and $4f$ are weakly populated. The situation is similar in the lower spectrum (hydrogen target), both for $n=4$ and 5 . From Table I, it is clear that branching ratios favor the fastest decay. Thus $(\Delta n)_{\text{max}}$ transitions occur and are the reason for weak transitions from $n=4$ in $\text{S}^{7+} + \text{H}_2$, where $n=5$ is mostly populated with substate population peaking at $5p$ and $5s$. (For the hydrogen case, the weak $4f-5g$ yrast transitions are found on the lower spectrum in Fig. 2.) Such behavior suggests that rotational coupling of these states is still weak at the projectile velocity studied here ($v \sim 0.29$ a.u.). Furthermore, the present system exhibits a behavior similar in some respects to the Ar^{7+} -on-helium case where capture was observed to populate mostly $n=4$ with a population share of the order of 50% going to p substates.⁸

The identification of transitions following double capture based on known data¹⁴ and consistency checks raises some questions discussed below.

For $\text{S}^{7+} + \text{He}$ or H_2 , according to the multiple-capture model of Bárány *et al.*,¹⁸ it is estimated that double capture from He would populate mostly $n=3, n'=3, 4$, and for H_2 targets, $n=4, n'=4, 5$. These doubly excited states lie high above the ionization limit and most are autoionizing. The fraction that stabilizes radiatively appears in the normal 2L sodiumlike S VI spectrum. Cascading terminates in the resonance doublet $3s {}^2S_{1/2} - 3p {}^2P_{1/2,3/2}$, which is expected to be the most intense transition. The $3p {}^2P_{1/2,3/2} - 3d {}^2D_{3/2,5/2}$ line is clearly identified and is weaker than the resonance transition. These two transitions are thus expected to be the most intense ones in the S VI spectrum. This raises some doubts, despite a wavelength coincidence with known lines, as to the identification of the 465 \AA line whose intensity exceeds that of the resonance transition, as well as of the one at 328.5 \AA for which not only is the intensity anomalous but the high angular momentum of the upper state ($5f$) is questionable.

V. CONCLUSION

We have shown that in charge-exchange collisions involving S^{7+} at low velocity, identification of unknown transitions and levels was possible. Further work is underway to clarify the questions raised above in other systems having equally complex structures.

ACKNOWLEDGMENTS

The calculations were carried out on the NAS9080 of the Centre Interrégional de Calcul Electronique (CIRCE, Orsay, France). We wish to thank NATO for Research

Grant No. 682/84, which facilitated collaborative aspects of this work. Thanks are due also to Christer Jupén (Lund) for communicating unpublished results on S VII, and to Joanne Miller, Norman Schlader, and Serge Knystautas for their assistance in the data reduction.

-
- ¹R. C. Isler, L. E. Murray, G. C. Crume, C. E. Bush, J. L. Dunlap, P. H. Edmonds, S. Kasai, E. A. Lazarus, M. Murakami, G. H. Neilson, V. K. Paré, S. D. Scott, C. E. Thomas, and A. J. Wootton, *Nucl. Fusion* **23**, 1017 (1983).
- ²U. Feldman, J. F. Seely, and G. A. Doschek, *J. Phys. (Paris) Colloq.* **47**, C6-187 (1986).
- ³E. Ya. Kononov, A. E. Kramida, L. I. Podobedova, E. N. Ragozin, and V. A. Chirkov, *Phys. Scr.* **28**, 496 (1983).
- ⁴C. Jupén, U. Litzén, and A. Trigueiros, *Phys. Scr.* **29**, 317 (1984).
- ⁵H. P. Garnir, Y. Baudinet-Robinet, P. D. Dumont, and M. Eidelsberg, *Phys. Scr.* **17**, 463 (1978).
- ⁶C. Jupén (private communication to S.B.).
- ⁷P. Marseille, S. Bliman, J.-P. Desclaux, S. Dousson, and D. Hitz, *J. Phys. B* **20**, 5127 (1987); P. Marseille, S. Bliman, P. Indelicato, and D. Hitz, *ibid.* **20**, L423 (1987).
- ⁸M.-G. Suraud, J.-J. Bonnet, M. Bonnefoy, M. Chassevent, A. Fleury, S. Bliman, S. Dousson, and D. Hitz, *J. Phys. B* **21**, 1219 (1988).
- ⁹M. Mayo, D. Hitz, M. Druetta, S. Dousson, J. P. Desclaux and S. Bliman, *Phys. Rev. Lett.* **54**, 317 (1985).
- ¹⁰R. Geller and B. Jacquot, *Phys. Scr.* **T3**, 63 (1983).
- ¹¹W. Eissner, M. Jones, and H. Nussbaumer, *Comput. Phys. Commun.* **8**, 270 (1974).
- ¹²M. Cornille, J. Dubau, F. Bely-Dubau, S. Bliman, D. Hitz, M. Mayo, J.-J. Bonnet, M. Bonnefoy, M. Chassevent, and A. Fleury, *J. Phys. B* **19**, L393 (1986).
- ¹³R. D. Cowan and K. L. Andrew, *J. Opt. Soc. Am.* **55**, 502 (1965).
- ¹⁴R. L. Kelly, Oak Ridge National Laboratory Report No. 5922, 1982 (unpublished).
- ¹⁵R. Mann, F. Folkmann, and H. F. Beyer, *J. Phys. B* **14**, 1161 (1981).
- ¹⁶S. Bliman, M.-G. Suraud, D. Hitz, J.-E. Rubensson, J. Nordgren, M. Cornille, P. Indelicato, and E. J. Knystautas, *J. Phys. B* **22**, 3647 (1989).
- ¹⁷C. Jupén, L. Engstrom, R. Hutton, and E. Träbert, *J. Phys. B* **21**, L347 (1988).
- ¹⁸A. Bárány, G. Astner, H. Cederquist, H. Danared, S. Hult, P. Hvelplund, A. Johnson, H. Knudsen, L. Liljeby, and K.-G. Rensfelt, *Nucl. Instrum. Methods B* **9**, 397 (1985).